

Electronic Supporting Material

Thermodynamics of Multilayer Protein Adsorption on Gold Nanoparticle Surface

Akriti Mishra and Puspendu Kumar Das*

Department of Inorganic and Physical Chemistry

Indian Institute of Science, Bangalore 560012, India

E-mail: pkdas@iisc.ac.in

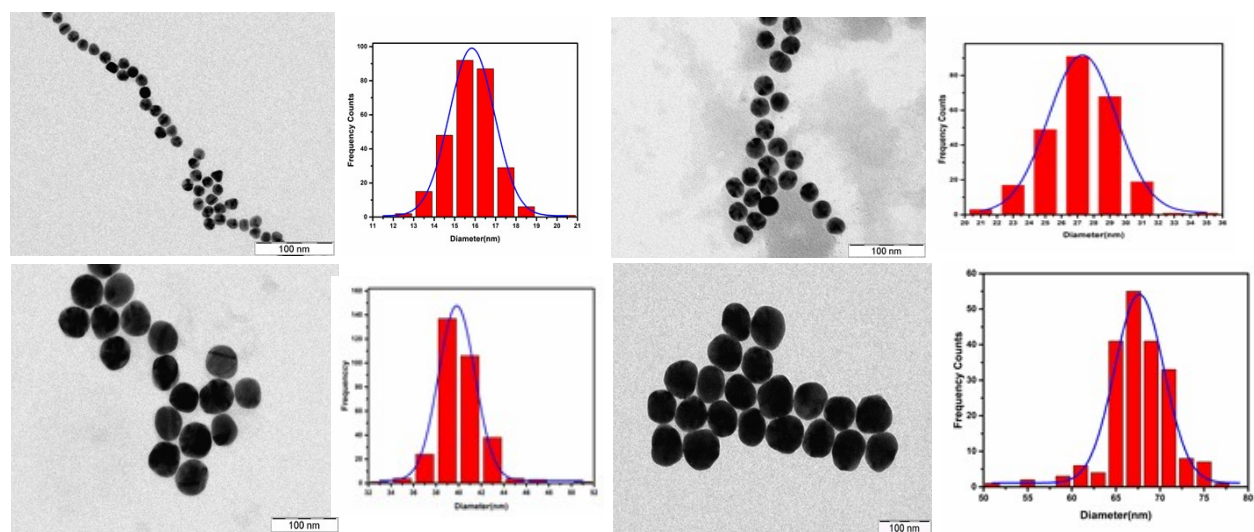


Figure S1. TEM images of 16 nm (15.8 ± 1.1 nm), 27 nm (27.3 ± 2.1 nm), 41 nm (41.0 ± 2.5 nm), and 69 nm (69.2 ± 2.7 nm) GNPs. The histograms show size distribution after analysing more than 350 particles. The ellipticity index (ratio of axes) varies from 0.92 to 1.06 suggesting that for GNPs of sizes 16 nm to 69 nm are of spherical shape.

The TEM diameter was considered as a reference to determine the concentration of synthesized GNPs following the method reported by Liu et al.⁴⁹ A calibration plot between the TEM diameter against the molar extinction coefficient was then utilized to obtain the concentration of GNPs.

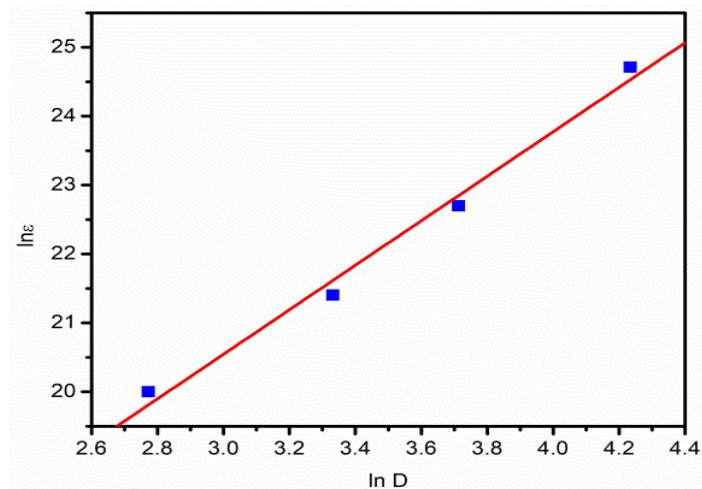


Figure S2. A log-log plot of molar extinction coefficient vs. GNP diameter (D in nm). Error bars are not visible in the log-log plot.

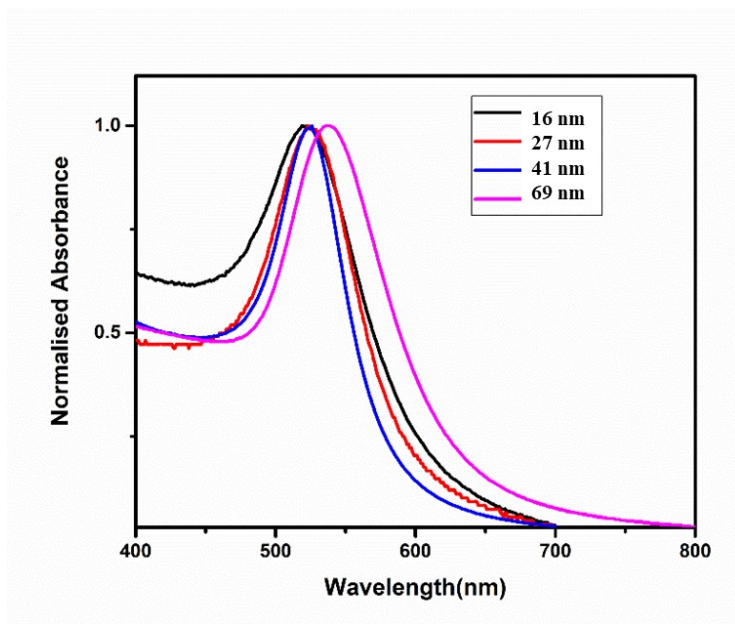


Figure S3. Absorption spectra of 16 nm, 27 nm, 41 nm, and 69 nm GNPs in 5 mM PB at pH 7.

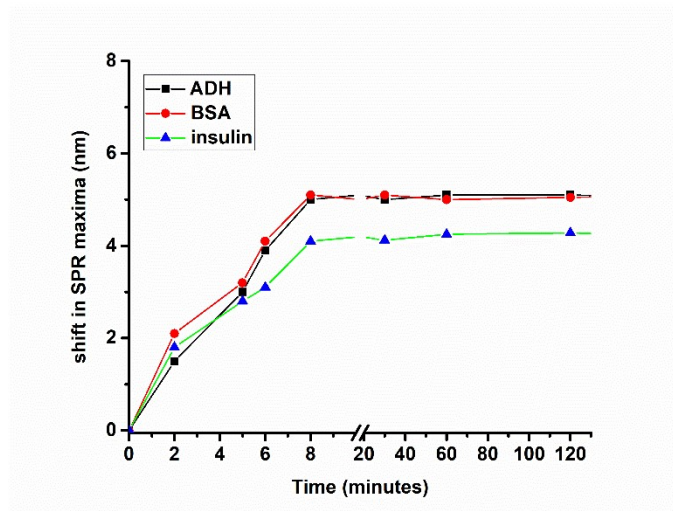


Figure S4. Shift in SPR maximum wavelength (nm) for 69 nm GNP at the endpoint of DLS experiments with time, where protein concentrations were 900 nM for ADH, 1200 nM BSA and 580 nM for insulin, respectively.

The extinction spectra of GNPs were recorded after addition of protein once the equilibrium was attained. The spectra do not show any new peak at the longer wavelength region after addition of protein leading to the conclusion that there was no aggregation of GNPs in the presence of proteins.

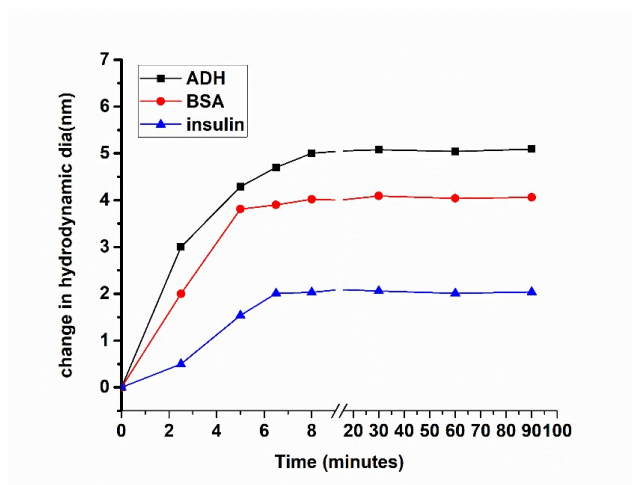


Figure S5: Change in the hydrodynamic diameter with time after addition of first aliquot of protein to 69 nm GNP solution (where protein concentrations being 24 nM for ADH, 24 nM and BSA, and 16 nM for insulin, respectively) in 5mM PB.

DLS intensity weighted size distribution profiles

The hydrodynamic diameter of the GNPs in solution was obtained from the intensity distribution function presented in Figure S6 for 16 nm and 69 nm. Similar observations were seen for 27 nm and 41 nm GNPs after adsorption of ADH, BSA and insulin.

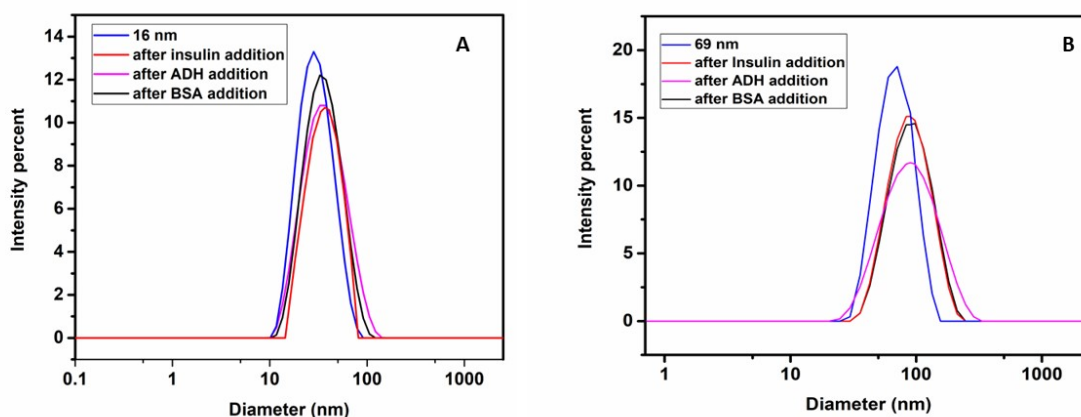


Figure S6. Intensity distribution profiles after ADH, BSA and insulin adsorption on (A) 16 nm, (B) 69 nm GNPs in 5 mM PB.

Table S1. Polydispersity index (PDI) values obtained at the endpoint of DLS experiments after protein addition.

GNP size	PDI	PDI after ADH adsorption	PDI after BSA adsorption	PDI after insulin adsorption
16 nm	0.34	0.30	0.28	0.31
27 nm	0.25	0.21	0.24	0.20

41 nm	0.22	0.18	0.21	0.20
69 nm	0.17	0.15	0.14	0.16

Comparison plot between Modified Langmuir model (MLM) and BET adsorption profiles

We have fitted one set of representative data for ADH adsorption on 41 nm GNP using MLM²¹ and BET model described in this paper. Similar fits were observed for all different GNPs.

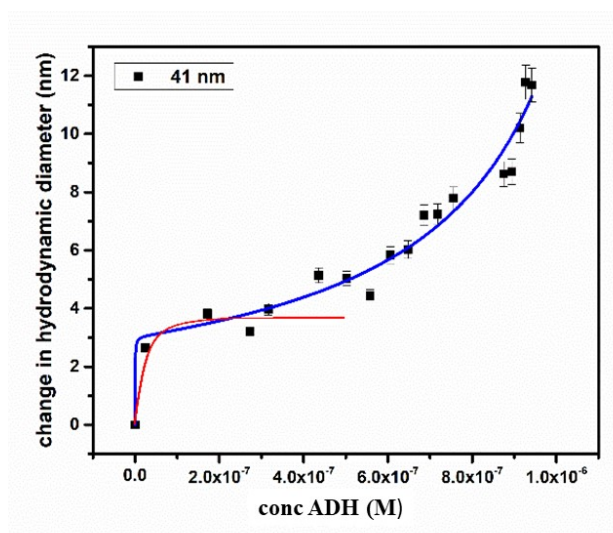


Figure S7. BET (blue) and MLM (red) fits for 41 nm GNP after ADH adsorption in 5 mM PB at 298 K. Error bars were calculated from three independent experiments.

Table S2. Zeta potential (ZP) values obtained after protein adsorption on GNPs at 298 K. Error bars are statistical average from three independent measurements

GNP size (nm)	ZP (mV)	ZP (mV) after ADH addition	ZP (mV) after BSA addition	ZP (mV) after insulin addition
16	-24.6 ± 3.8	-17.4 ± 3.0	-19.4 ± 3.5	-18.2 ± 4.5
27	-42.7 ± 4.2	-34.1 ± 3.0	-33.7 ± 3.0	-38.3 ± 5.0

41	-54.3 ± 5.2	-33.8 ± 4.0	-38.4 ± 4.0	-40.3 ± 5.0
69	-58.0 ± 4.7	-29.4 ± 2.0	-39.6 ± 3.0	-43.6 ± 6.0

Dislodging hard and soft protein corona from the GNP surface

The GNP-PC studied in this paper were centrifuged at speeds of 15000 rpm for 16 nm, 9000 rpm for 27 nm, 6000 rpm for 41 nm, and 4000 rpm for 69 nm for a duration of 30 minutes. The supernatant was removed and the GNPs in the bottom of the centrifuge tube were redispersed in mQ water. The hydrodynamic size of the resulting GNPs was determined from DLS studies. The measured size was close to the initial size of the GNPs before protein adsorption as shown in Table S3. It leads us to conclude that both the soft and ultrasoft corona are rather weakly bound on the GNP surface and can be dislodged from the surface by centrifugation.

Table S3. Change in the hydrodynamic size (Δ) of GNPs after centrifugation of GNP-protein conjugate at desired rpm with the initial hydrodynamic size of GNPs before protein addition.

GNP size (nm)	Δ (nm) after centrifugation for ADH addition	Δ (nm) after centrifugation for BSA addition	Δ (nm) after centrifugation for insulin addition
16	0.8 ± 0.4	0.7 ± 0.4	1.1 ± 0.4
27	0.8 ± 0.5	1.1 ± 0.5	1.0 ± 0.6
41	1.0 ± 0.3	1.0 ± 0.4	1.1 ± 0.4
69	1.1 ± 0.6	1.0 ± 0.4	1.0 ± 0.7

Stability of proteins with temperature

1 mL of each protein having a fixed concentration in 5 mM PB was taken in a quartz cuvette and the scattering at a fixed wavelength and temperature was recorded as a function of time. The cuvette temperature is increased in steps of 5K and the corresponding change in the Rayleigh scattering intensity at 340 nm is monitored till 318 K. As shown in figure S8, the Rayleigh scattering intensities did not change significantly suggesting that the proteins are stable in the 283-318 K temperature range.

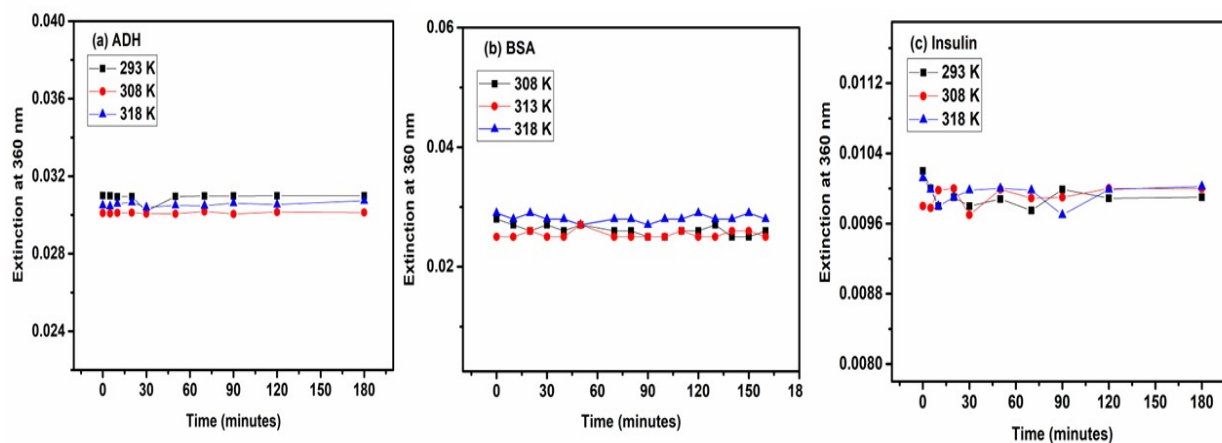


Figure S8. Rayleigh scattering intensity at 340 nm as a function of time for (a) 5 μ M ADH, (b) 10 μ M BSA, and (c) 1.5 μ M insulin at different temperatures.

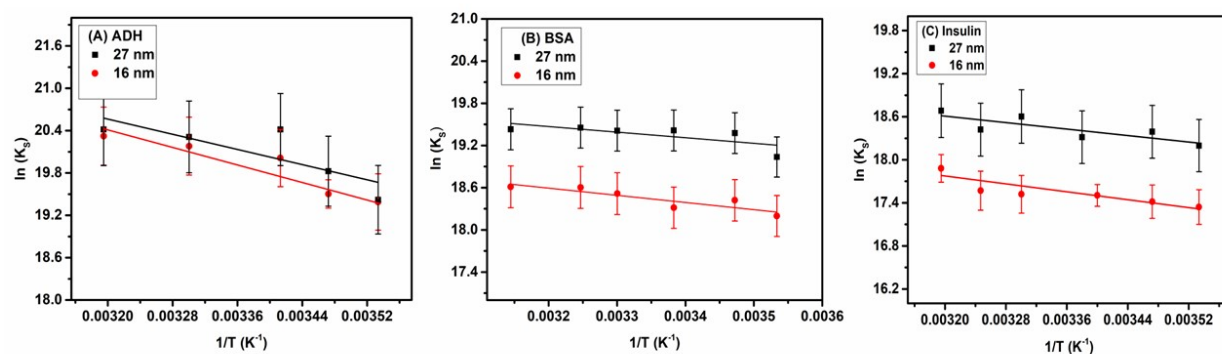


Figure S9. Van't Hoff plots for (a) ADH, (b) BSA, and (c) insulin binding on 16 and 27 nm GNPs. The straight lines through the experimental data points are fitted using the least squares

method. Error bars are calculated from three independent experiments. The R^2 values for the linear fit vary from 0.52-0.74 which show that the fits are not very good.